

Decentralized Entropic Optimal Transport for Privacy-preserving Distributed Distribution Comparison

Xiangfeng Wang¹ Hongteng Xu² Moyi Yang^{1*}

¹School of Computer Science and Technology, East China Normal University

²Gaoling School of Artificial Intelligence, Renmin University of China

xfwang@sei.ecnu.edu.cn hongtengxu@ruc.edu.cn winnie_yang@stu.ecnu.edu.cn

January 31, 2023

Abstract

Privacy-preserving distributed distribution comparison measures the distance between the distributions whose data are scattered across different agents in a distributed system and cannot be shared among the agents. In this study, we propose a novel decentralized entropic optimal transport (EOT) method, which provides a *privacy-preserving* and *communication-efficient* solution to this problem with theoretical guarantees. In particular, we design a mini-batch randomized block-coordinate descent (MRBCD) scheme to optimize the decentralized EOT distance in its dual form. The dual variables are scattered across different agents and updated locally and iteratively with limited communications among partial agents. The kernel matrix involved in the gradients of the dual variables is estimated by a distributed kernel approximation method, and each agent only needs to approximate and store a sub-kernel matrix by one-shot communication and without sharing raw data. We analyze our method’s communication complexity and provide a theoretical bound for the approximation error caused by the convergence error, the approximated kernel, and the mismatch between the storage and communication protocols. Experiments on synthetic data and real-world distributed domain adaptation tasks demonstrate the effectiveness of our method.

1 Introduction

Distribution comparison plays a central role in many machine learning problems, such as data clustering (Hammouda & Karray, 2000), generative modeling (Bond-Taylor et al., 2021; Mattei & Frellsen, 2019), domain adaptation (Ganin & Lempitsky, 2015; Farahani et al., 2020), etc. As a valid metric for distributions, optimal transport (OT) distance (Villani, 2009) provides a powerful solution to this task. Given two distributions, the optimal transport distance corresponds to the minimum expectation of their underlying sample distance. The corresponding optimal joint distribution of sample pairs takes these two distributions as its marginals. Mathematically, given two probability measures in a compact space \mathcal{X} , denoted as $\mu, \gamma \in \mathcal{P}(\mathcal{X})$, the Kantorovich formulation of the optimal transport distance between them is defined as

$$W(\mu, \gamma) \stackrel{\text{def.}}{=} \inf_{\pi \in \Pi(\mu, \gamma)} \int_{\mathcal{X}^2} c(x, y) \, d\pi(x, y), \quad (1)$$

*The authors have equal contributions and are listed in alphabetical order of their last names.

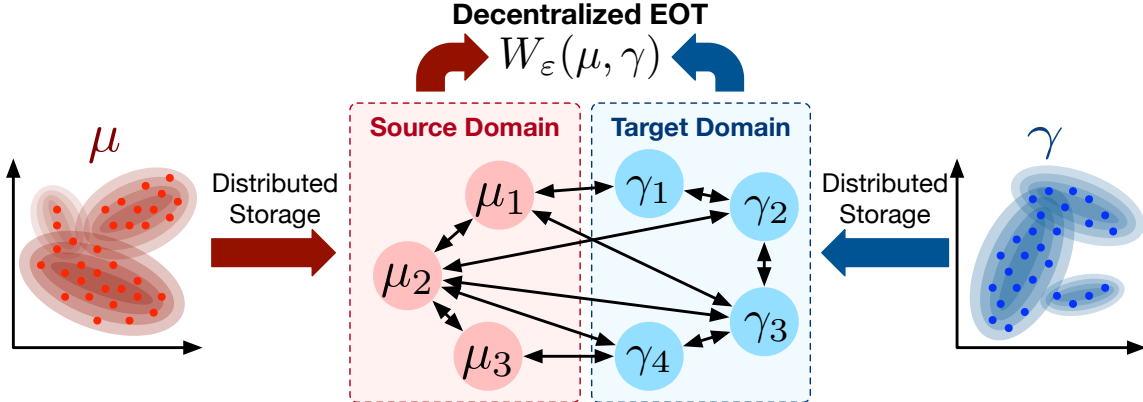


Figure 1: An illustration of the privacy-preserving distributed distribution comparison task and the corresponding decentralized entropic optimal transport problem. To emphasize, the data in two domains obey the distribution μ and γ , respectively, but are scattered among different agents. Each agent merely contains a part of samples, and the local distribution is denoted as μ_i (or γ_j).

where $c : \mathcal{X}^2 \mapsto [0, \infty)$ denotes a continuous cost function, the joint distribution on the product space $\mathcal{X} \times \mathcal{X}$ is denoted as the coupling π , and $\Pi(\mu, \gamma) = \{\pi \in \mathcal{P}(\mathcal{X} \times \mathcal{X}) \mid \forall (\mathcal{A}, \mathcal{B}) \subset \mathcal{X} \times \mathcal{X}, \pi(\mathcal{A} \times \mathcal{X}) = \mu(\mathcal{A}), \pi(\mathcal{X} \times \mathcal{B}) = \gamma(\mathcal{B})\}$ denotes the marginal constraints of the coupling. The OT distance is applicable even if the supports of the two distributions are non-overlapped. Therefore, leveraging it to fit a model distribution to the data distribution (Arjovsky et al., 2017; Deshpande et al., 2018) or transferring a source distribution to a target one (Courty et al., 2014; Damodaran et al., 2018) usually leads to encouraging performance.

In practice, the optimal transport distance in equation 1 is often implemented with an entropic regularizer (Cuturi, 2013; Blondel et al., 2018), which leads to a strictly-convex optimization problem called entropic optimal transport (EOT):

$$W_\varepsilon(\mu, \gamma) \stackrel{\text{def.}}{=} \inf_{\pi \in \Pi(\mu, \gamma)} \int_{\mathcal{X}^2} c(x, y) d\pi(x, y) - \varepsilon H(\pi), \quad (2)$$

where $H(\pi) = - \int_{\mathcal{X} \times \mathcal{X}} \pi(x, y) \log(\pi(x, y) - 1) dx dy$ denotes the entropy of π . Given the samples of μ and γ , this problem can be solved more efficiently using alternate minimization schemes, e.g., the Sinkhorn algorithm (Cuturi, 2013) and its stochastic version (Altschuler et al., 2017), the primal-dual method (Blondel et al., 2018), and the block-coordinate descent method (Genevay et al., 2016). These algorithms are centralized in general – a central server records all pairwise costs, i.e., $C = [c(x, y)]$, and optimizes the objective accordingly.

However, the samples in many real-world applications are often large-scale and scattered across different agents in a distributed and decentralized system (i.e., each agent only has limited storage and computation power, and none works as a central server). In addition, sharing raw data directly can be forbidden in this system because of privacy and security requirements. As illustrated in Figure 1, such a scenario leads to a challenging *privacy-preserving distributed distribution comparison* task, in which each agent can access neither the whole sample sets nor the complete cost matrix C . Accordingly, a decentralized method is required to solve the EOT problem with limited and privacy-preserving communications.

In this study, we propose a novel decentralized entropic optimal transport method, which provides a theoretically-guaranteed solution to privacy-preserving distributed distribution comparison. In particular, our method considers the dual form of the EOT problem, in which the dual objective

involves a kernel associated with the cost matrix, and the dual variables are scattered among the agents. We approximate a sub-kernel matrix for each agent via one-shot communication and avoid sharing raw data among the agents (Khanduri et al., 2021). Based on the approximated kernel, the dual variables are optimized in a mini-batch randomized block-coordinate descent (MRBCD) scheme (Zhao et al., 2014). Each agent stores and updates the dual variables corresponding to its local data. The dual variables’ gradients are computed based on partial dual variables (rather than raw data) from some randomly-selected agents.

Our method is privacy-preserving and communication-efficient because the communications do not contain raw data, and the communication cost is independent of the data dimension. Moreover, as our main theoretical contribution, we make the first attempt to provide an error bound of decentralized EOT distance caused by the convergence error, the kernel approximation error, and the mismatch between the distributed system’s storage and communication protocols. Experiments on synthetic data verify the effectiveness of our method and its robustness to hyperparameters and communication protocols. Furthermore, we test our decentralized EOT in real-world distributed domain adaptation tasks, demonstrating its usefulness for privacy-preserving distributed distribution comparison.

2 Related Work

2.1 Entropic optimal transport methods

Typically, the entropic optimal transport distance can be solved by the Sinkhorn algorithm (Sinkhorn & Knopp, 1967; Cuturi, 2013; Benamou et al., 2015) (or its logarithmic variant (Chizat et al., 2018; Schmitzer, 2019) for improving numerical stability). Following the Sinkhorn algorithm, the method in (Xie et al., 2020) computes the OT distance via an inexact proximal point algorithm, which is equivalent to solving an EOT problem with a temporally-decayed entropic regularizer. The Greenkhorn algorithm (Altschuler et al., 2017) works as a stochastic Sinkhorn algorithm with significant computation efficiency. Besides the Sinkhorn algorithm, some other efficient algorithms are developed, e.g., the Bregman alternating direction method of multipliers (Bregman ADMM) (Wang & Banerjee, 2014a; Ye et al., 2017), smoothed semi-dual algorithm (Blondel et al., 2018), and conditional gradient algorithm (Titouan et al., 2019). The work in (Genevay et al., 2016; Seguy et al., 2018) introduce stochastic optimization mechanisms into the large-scale optimal transport problem.

The above methods mainly focus on the EOT problems in centralized scenarios. The decentralized EOT is seldom studied. Recently, the work in (Zhang & Zhu, 2019; Hughes & Chen, 2021) proposes some ADMM-based decentralized algorithms for distributed resource allocation tasks. The formulation of their tasks is relevant to an optimal transport problem rather than an EOT problem. Moreover, unlike our work, their methods neither apply any privacy-preserving mechanism nor consider the mismatch between the distributed system’s storage and communication protocols. Additionally, the decentralized EOT problem differs from the well-known distributed and decentralized Wasserstein barycenter problems Staib et al. (2017); Uribe et al. (2018); Dvurechenskii et al. (2018). In these barycenter problems, the samples of a distribution are still stored in a single agent so that the (entropic) optimal transport distance between the distribution and the barycenter can still be computed in a centralized manner. On the contrary, in our study, each agent can only access a part of the distribution samples and cannot share them with other agents, so we need a decentralized algorithm to compute the EOT distance.

2.2 Distributed and decentralized optimization

Distributed and decentralized optimization methods can be broadly divided into primal and primal-dual types (Nedic & Ozdaglar, 2009; Duchi et al., 2011). Primal methods usually refer to gradient-based methods such as decentralized gradient descent (DGD) (Yuan et al., 2016; Lobel & Ozdaglar, 2010), EXTRA (Shi et al., 2015), etc. For large-scale optimization tasks, the stochastic gradient technique is often applied, e.g., the decentralized stochastic gradient descent method (DSGD) (Agarwal & Duchi, 2011) is generalized from the DGD, with significant computational efficiency acceleration. The primal-dual approaches further employ dual variables to design distributed optimization methods, which incorporate distributed dual decomposition (Terelius et al., 2011), ADMM (Chang et al., 2015; Shi et al., 2014), etc. More discussions can refer to a series of survey papers (Chang et al., 2020; Nedic, 2020; Assran et al., 2020).

Besides computational efficiency, communication efficiency is also required for distributed and decentralized optimization. The most intuitive way to increase the communication efficiency is to reduce the number of agents involved in communications (Smith et al., 2018), e.g., the random node selection scheme (Arablouei et al., 2015; Mao et al., 2020) and the importance sampling scheme (Chen et al., 2018; Liu et al., 2019). To reduce the bandwidth, the information for each communication is often compressed by sparsification (Stich et al., 2018; Basu et al., 2019; Tang et al., 2020) or quantization (Zhu et al., 2016; Alistarh et al., 2017; Zhang et al., 2019; Lu & De Sa, 2020). Recently, the distributed and decentralized optimization techniques have been utilized for distributed deep learning (Tang et al., 2020), distributed edge AI system (Shi et al., 2020), federated learning (Chen et al., 2021), etc. As aforementioned, these applications often involve privacy-preserving distributed distribution comparison, which motivates us to develop the decentralized EOT method with privacy preservation and communication efficiency.

3 Proposed Algorithm Framework

3.1 Dual formulation of decentralized EOT

Suppose that there are I agents in the source domain storing the samples of μ and J agents in the target domain storing the samples of γ , as illustrated in Figure 1. The distribution of the samples in the i -th source agent (the j -th target agent) is denoted as μ_i (γ_j). Accordingly, the storage of the samples in the agents can be captured by the following hierarchical model:

$$\begin{aligned} \text{Agent selection: } & i \sim p, \quad j \sim q, \\ \text{Sample assignment: } & X_i = \{x_n^{(i)}\}_{n=1}^{N_i} \sim \mu_i, \quad Y_j = \{y_m^{(j)}\}_{m=1}^{M_j} \sim \gamma_j, \end{aligned} \tag{3}$$

where $p = \{p_i\}_{i=1}^I \in \Delta^{I-1}$ and $q = \{q_j\}_{j=1}^J \in \Delta^{J-1}$, respectively. p_i (q_j) represents the probability of selecting the source agent i (the target agent j) to store the corresponding data. $X_i = \{x_n^{(i)}\}_{n=1}^{N_i}$ and μ_i denote the samples stored in the agent i and the corresponding sample distribution. $Y_j = \{y_m^{(j)}\}_{m=1}^{M_j}$ and γ_j are denoted in the same way. Obviously, we have $\mu = \sum_i p_i \mu_i$, $\gamma = \sum_j q_j \gamma_j$, $X = \{x_n\}_{n=1}^N = \cup_i X_i$, and $Y = \{y_m\}_{m=1}^M = \cup_j Y_j$.

- **Storage Protocol.** Sampling source and target agents independently from p and q is equivalent to sampling the agent pairs from the distribution $p \otimes q = [p_i q_j]$. Here, we define $p \otimes q$ as the *storage protocol* of the distributed system.

Taking the storage protocol and the Fenchel dual form of the EOT distance (Peyré & Cuturi, 2019) into account, we rewrite the EOT distance in equation 2 as follows:

$$\begin{aligned} W_\varepsilon(\mu, \gamma) &= \sup_{u, v \in \mathcal{C}_\mathcal{X}} \int_{\mathcal{X}} u(x) d\mu(x) + \int_{\mathcal{X}} v(y) d\gamma(y) - \varepsilon \int_{\mathcal{X}^2} e^{\frac{u(x)+v(y)-c(x,y)}{\varepsilon}} d\mu(x)d\gamma(y) \\ &= \sup_{u, v \in \mathcal{C}_\mathcal{X}} \mathbb{E}_{x \sim \mu, y \sim \gamma} f_\varepsilon(x, y, u, v) \\ &= \sup_{u, v \in \mathcal{C}_\mathcal{X}} \mathbb{E}_{(i,j) \sim p \otimes q} \mathbb{E}_{x \sim \mu_i, y \sim \gamma_j} f_\varepsilon(x, y, u, v). \end{aligned} \quad (4)$$

Here, $\mathcal{C}_\mathcal{X}$ represents the set of continuous functions defined in \mathcal{X} , $u, v \in \mathcal{C}_\mathcal{X}$ denote the dual functions, which are also called Kantorovich potentials, and

$$f_\varepsilon(x, y, u, v) = u(x) + v(y) - \varepsilon e^{\frac{u(x)+v(y)}{\varepsilon}} \underbrace{e^{-\frac{c(x,y)}{\varepsilon}}}_{\kappa(x,y)}, \quad (5)$$

where $\kappa(x, y)$ is a kernel function associated with the cost $c(x, y)$. The second equation in equation 4 indicates that the EOT problem can be modeled as an unconstrained expectation maximization problem with respect to u and v (Genevay et al., 2016). The third equation in equation 4 is based on the hierarchical model in equation 3.

- **Communication Protocol.** As shown in equation 4, computing the EOT distance requires us to sample agent pairs based on the storage protocol. In practice, however, the sampling of the agent pairs is determined by the *communication protocol* rather than the storage protocol of the distributed system. Here, we define the communication protocol as the distribution of the communicable agent pairs, denoted as $E = [e_{ij}] \in \{E \in \mathbb{R}_+^{I \times J} \mid \mathbf{1}_I^\top E \mathbf{1}_J = 1\}$.

Note that, the communication protocol can be mismatched with the storage protocol. For example, some systems do not allow multi-step routes and/or restrict the communication between the agents to be directed, which may cause $E \neq p \otimes q$. As a result, we actually approximate $W_\varepsilon(\mu, \gamma)$ by the following surrogate:

$$\widetilde{W}_\varepsilon(\mu, \gamma) \stackrel{\text{def.}}{=} \sup_{u, v \in \mathcal{C}_\mathcal{X}} \mathbb{E}_{(i,j) \sim E} \mathbb{E}_{x \sim \mu_i, y \sim \gamma_j} f_\varepsilon(x, y, u, v). \quad (6)$$

In theory, the gap between $\widetilde{W}_\varepsilon(\mu, \gamma)$ and $W_\varepsilon(\mu, \gamma)$ is bounded under mild assumptions:

Theorem 1. Let $\mu = \sum_i p_i \mu_i$ and $\gamma = \sum_j q_j \gamma_j$ be the two distributions in a distributed system with I source agents and J target agents, whose storage and communication protocols are $p \otimes q = [p_i q_j]$ and $E = [e_{ij}]$, respectively. Let $\max_{i,j} W_\varepsilon(\mu_i, \gamma_j) \leq \tau$ for some $\tau > 0$ and $\sum_{i,j} |e_{ij} - p_i q_j| \leq \sigma$ for some $\sigma > 0$. We have

$$|\widetilde{W}_\varepsilon(\mu, \gamma) - W_\varepsilon(\mu, \gamma)| \leq \tau \sigma. \quad (7)$$

Theorem 1 indicates that as long as the mismatch between the storage and communication protocols (i.e., σ) is small, we can approximate $W_\varepsilon(\mu, \gamma)$ well by $\widetilde{W}_\varepsilon(\mu, \gamma)$.¹ Ideally, $\widetilde{W}_\varepsilon(\mu, \gamma) = W_\varepsilon(\mu, \gamma)$ when $E = p \otimes q$. Fortunately, this ideal case can be available in many situations. For example, in a distributed system built on a connected network and with a known storage protocol, we can first select a source agent based on p and then select a target agent based on q (so that $E = p \otimes q$). In more general settings, we often can adjust the communication protocol, matching it with the storage protocol as much as possible.

¹Theorem 1 is valid for both continuous probability measures and sample-based discrete measures.

Given the samples of μ and γ , the problem in equation 6 becomes

$$\max_{\substack{u=\{u^{(i)}\}_{i=1}^I \in \mathbb{R}^N \\ v=\{v^{(j)}\}_{j=1}^J \in \mathbb{R}^M}} \overbrace{\sum_{i=1}^I \sum_{j=1}^J \frac{e_{ij}}{N_i M_j} f_\varepsilon(K_{ij}, u^{(i)}, v^{(j)})}^{F_\varepsilon(u, v; K, E)}, \quad (8)$$

where the dual functions $u(x)$ and $v(y)$ become the dual variables $u \in \mathbb{R}^N$ and $v \in \mathbb{R}^M$, respectively. The dual objective $F_\varepsilon(u, v; K, E)$ takes the kernel matrix $K = [\kappa(x_n, y_m)] \in \mathbb{R}^{N \times M}$ and the communication protocol E as its hyperparameters. The dual objective is decomposable — for the agent pair (i, j) , $f_\varepsilon^{(i,j)} = \sum_{n=1}^{N_i} \sum_{m=1}^{M_j} f_\varepsilon(\kappa(x_n^{(i)}, y_m^{(j)}), u_n^{(i)}, v_m^{(j)}) = u_n^{(i)} + v_m^{(j)} - \varepsilon \exp(\frac{u_n^{(i)} + v_m^{(j)}}{\varepsilon}) \kappa(x_n^{(i)}, y_m^{(j)})$ is the corresponding local objective, in which $K_{ij} = [\kappa(x_n^{(i)}, y_m^{(j)})] \in \mathbb{R}^{N_i \times M_j}$ is a block of K . Moreover, each local objective only involves a part of dual variables that correspond to the local samples stored in the agents, e.g., the $u^{(i)} = [u_n^{(i)}] \in \mathbb{R}^{N_i}$ in $f_\varepsilon^{(i,j)}$ corresponds to the samples $\{x_n^{(i)}\}_{n=1}^{N_i}$ in the source agent i . As a result, the dual variables can be scattered across different agents, and accordingly, the gradient of $u^{(i)}$ can be formulated as follows:

$$\nabla_{u^{(i)}} F_\varepsilon(u, v; K, E) = \sum_{j=1}^J \frac{e_{ij}}{N_i M_j} \nabla_{u^{(i)}} f_\varepsilon^{(i,j)} = \sum_{j=1}^J \frac{e_{ij}}{N_i M_j} \begin{bmatrix} \sum_{m=1}^{M_j} 1 - e^{\frac{u_1^{(i)} + v_m^{(j)}}{\varepsilon}} \kappa(x_1^{(i)}, y_m^{(j)}) \\ \vdots \\ \sum_{m=1}^{M_j} 1 - e^{\frac{u_{N_i}^{(i)} + v_m^{(j)}}{\varepsilon}} \kappa(x_{N_i}^{(i)}, y_m^{(j)}) \end{bmatrix}. \quad (9)$$

The gradient in equation 9 points out the challenges of the proposed decentralized EOT problem. In particular, when computing the gradient of $u^{(i)}$, we need to transmit the raw data and the dual variables of all the agents in the other domain to the agent i . The communication cost of this step is high, especially for high-dimensional data. Moreover, sharing raw data results in the leakage of private information. Facing the above challenges, in the following subsection, we will introduce a decentralized EOT method to solve equation 8 in a privacy-preserving and communication-efficient way.

3.2 Proposed decentralized EOT method

The proposed decentralized EOT method consists of two steps: *i*) leveraging a theoretically-guaranteed method to approximate the kernel matrix without the share of raw data and *ii*) updating the dual variables locally and iteratively in a mini-batch randomized block-coordinate descent (MRBCD) scheme.

Privacy-preserving kernel approximation. When the cost $c(x, y)$ is Euclidean, the kernel $\kappa(x, y)$ in equation 5 is a special case of the following generalized inner product (GIP) kernel (Khanduri et al., 2021):

$$\kappa(x, y) = g(\phi(x, y), \|x\|, \|y\|), \quad (10)$$

where $\phi(x, y) = \arccos(\frac{\langle x, y \rangle}{\|x\| \|y\|})$, and $g(\phi, \|x\|, \|y\|)$ is a G -Lipschitz continuous function with respect to ϕ .

For the GIP kernel, it is possible to approximate it without the share of raw data (Khanduri et al., 2021). Denote D as the dimension of samples. Leveraging the random seed sharing method in (Xu et al., 2021; Richards et al., 2020), we can sample P D -dimensional random variables from a multivariate normal distribution, i.e., $\{\omega_\ell\}_{\ell=1}^P \sim \mathcal{N}(0, I_D)$, and broadcast them to all the agents.

Algorithm 1 Privacy-preserving Kernel Approximation

- 1: Draw random variables $\{\omega_\ell \in \mathbb{R}^D\}_{\ell=1}^P \sim \mathcal{N}(0, I_D)$ and broadcast them to all agents.
 - 2: **for** Each source agent $i \in \{1, \dots, I\}$ **do**
 - 3: Construct A_{μ_i} via equation 11 and broadcast it to all target agents. $\mathcal{O}(JN_i P)$
 - 4: If data is not normalized, broadcast $\{\|x_n^{(i)}\|\}_{n=1}^{N_i}$ to all target agents. $\mathcal{O}(JN_i)$
 - 5: **end for**
 - 6: **for** Each target agent $j \in \{1, \dots, J\}$ **do**
 - 7: Construct A_{γ_j} via equation 11 and broadcast it to all source agents. $\mathcal{O}(IM_j P)$
 - 8: If data is not normalized, broadcast $\{\|y_m^{(j)}\|\}_{m=1}^{M_j}$ to all source agents. $\mathcal{O}(IM_j)$
 - 9: **end for**
 - 10: Construct $\{\hat{K}_{ij}\}_{j=1}^J$ for each source agent i and $\{\hat{K}_{ij}\}_{i=1}^I$ for each target agent j via equation 12.
-

Based on the random variables, we can construct a binary matrix for each agent. Take the source agent i as an example. Given N_i samples $\{x_n^{(i)}\}_{n=1}^{N_i}$, we have

$$A_{\mu_i} = [\mathbb{I}(\langle \omega_\ell, x_n^{(i)} \rangle \geq 0)] \in \{0, 1\}^{P \times N_i}, \quad (11)$$

where $\mathbb{I}(\cdot)$ is an indicator, which outputs 1 if the input statement is true and outputs 0 otherwise. As a result, for each agent pair (i, j) , the kernel $\kappa(x_n^{(i)}, y_m^{(j)})$ of their samples can be approximated by

$$\hat{\kappa}(x_n^{(i)}, y_m^{(j)}) = g(\hat{\psi}(a_n^{(i)}, a_m^{(j)}), \|x_n^{(i)}\|, \|y_m^{(j)}\|) = g\left(\pi \left|1 - \frac{2}{P} \langle a_n^{(i)}, a_m^{(j)} \rangle\right|, \|x_n^{(i)}\|, \|y_m^{(j)}\|\right), \quad (12)$$

where $a_n^{(i)}$ is the n -th column of A_{μ_i} and $a_m^{(j)}$ is the m -th column of A_{γ_j} . Based on equation 12, we can obtain an approximated kernel matrix for an agent pair (i, j) , i.e., $\hat{K}_{ij} = [\hat{\kappa}(x_n^{(i)}, y_m^{(j)})]$. This approximation preserves data privacy because it only requires two constructed binary matrices and the norms of samples. The scheme of the privacy-preserving kernel approximation method is shown in Algorithm 1. The communication complexity of each step is shown in red.

As shown in Algorithm 1, by one-shot communication, each agent obtains the matrices A 's from all the agents in the other domain. Accordingly, the overall communication complexity is $\mathcal{O}((IM + JN)P)$. Note that, this complexity is independent with the sample dimension D , so it is suitable for high-dimensional cases. Moreover, even if $P = \mathcal{O}(N)$, the practical communication cost can still be tractable because the matrices A 's are binary and can be compressed before communication. The precision of the proposed approximation is guaranteed under mild assumptions:

- **Assumption 1.** The kernel in the objective is a GIP kernel, i.e., $\kappa(x, y) = g(\phi(x, y), \|x\|, \|y\|)$ and g is a G -Lipschitz continuous function with respect to ϕ .
- **Assumption 2.** Both the kernel κ and its approximation $\hat{\kappa}$ are bounded, i.e., $|\kappa(x, y)| \leq b$ and $|\hat{\kappa}(x, y)| \leq b$ for some $b \geq 1$.

Theorem 2. Let $K \in \mathbb{R}^{N \times M}$ be the matrix defined by the GIP kernel in equation 10 and \hat{K} be the approximation achieved via equation 12. Based on the assumptions 1-2, with probability at least $1 - \delta$, we have $\|K - \hat{K}\| \leq G(N + M) \left(\sqrt{\frac{32\pi^2}{P} \log \frac{2(N+M)}{\delta}} + \frac{8\pi}{3P} \log \frac{2(N+M)}{\delta} \right)$.

Theorem 2 means that $\hat{K} \rightarrow K$ when $P \rightarrow \infty$. $P = \mathcal{O}(\epsilon^{-2})$ achieves an approximation error $\epsilon > 0$. Theorem 2 is based on the Lemma 4.1 in (Khanduri et al., 2021). More details can be found at Appendix A.

Algorithm 2 MRBCD for Decentralized EOT Distance

- 1: For each source agent i and target agent j , construct $\{\hat{K}_{ij}\}_{j=1}^J$ and $\{\hat{K}_{ij}\}_{i=1}^I$ via Algorithm 1, and initialize $u^{(i)} = 0$ and $v^{(j)} = 0$. $\mathcal{O}((IM + JN)P)$
 - 2: **Update dual variables:** $\mathcal{O}(TL(\frac{N}{T} + \frac{M}{J}))$
 - 3: **for** $t = 0, 1, \dots, T$ **do**
 - 4: Set the learning rate $\eta_t = \frac{\eta}{\sqrt{t+1}}$.
 - 5: **for** An agent pair $(i, j) \sim E$ **do**
 - 6: Select L target agents $\mathcal{J}_L \sim \frac{1}{\|E[i, :]\|_1} E[i, :]$. Send $\{v^{(j),t}\}_{j \in \mathcal{J}_L}$ to the source agent i .
 - 7: $u^{(i),t+1} \leftarrow u^{(i),t} + \eta_t \sum_{j \in \mathcal{J}_L} \nabla_{u^{(i)}} \hat{f}_\varepsilon^{(i,j),t}$
 - 8: Select L source agents $\mathcal{I}_L \sim \frac{1}{\|E[:, j]\|_1} E[:, j]$. Send $\{u^{(i),t}\}_{i \in \mathcal{I}_L}$ to the target agent j
 - 9: $v^{(j),t+1} \leftarrow v^{(j),t} + \eta_t \sum_{i \in \mathcal{I}_L} \nabla_{v^{(j)}} \hat{f}_\varepsilon^{(i,j),t}$
 - 10: **end for**
 - 11: **end for**
 - 12: For an arbitrary source agent i , receive the optimal dual objectives $\{\{\hat{f}_\varepsilon^{(i',j)}\}_{j=1}^J\}_{i' \neq i}$ from the remaining agents in the source domain. $\mathcal{O}(IJ)$
 - 13: Compute $\tilde{W}_\varepsilon(\mu, \gamma)$ in the source agent i and broadcast it to all other agents. $\mathcal{O}(IJ)$
-

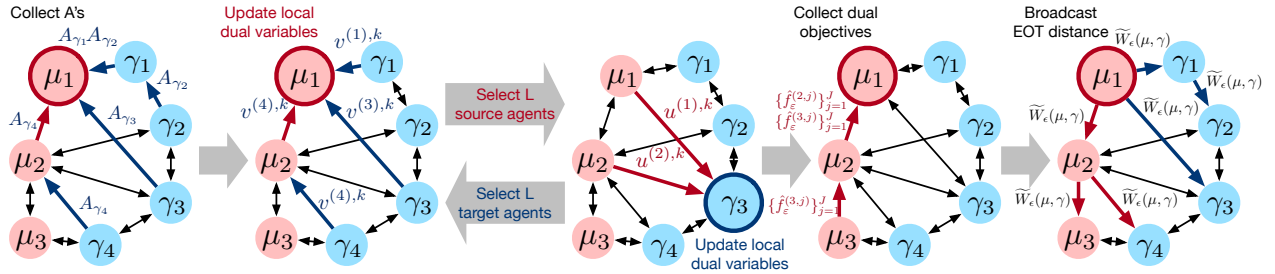


Figure 2: An illustration of the proposed decentralized EOT method.

Mini-batch randomized block-coordinate descent (MRBCD) scheme. Plugging the approximated kernel into equation 8, we denote the dual objective using the approximated kernel, i.e., $F_\varepsilon(u, v; \hat{K}, E) = \sum_{i,j} e_{ij} \hat{f}_\varepsilon^{(i,j)}$, where $\hat{f}_\varepsilon^{(i,j)} = f_\varepsilon(\hat{K}_{ij}, u^{(i)}, v^{(j)})$. Accordingly, we propose a mini-batch randomized block coordinate descent scheme, computing the gradient of $\hat{f}_\varepsilon^{(i,j)}$ based on a batch of agents and optimizing the decentralized EOT problem iteratively.

Take a source agent i as an example. In the t -th iteration, the agent i receives the dual variables $\{v^{(j),t}\}_{j \in \mathcal{J}_L}$ from L target agents, where $\mathcal{J}_L \subset \{1, \dots, J\}$ denotes the set of the L target agents. In practice, we sample \mathcal{J}_L based on the communication protocol E , i.e., $\mathcal{J}_L \sim \frac{1}{\|E_{i,:}\|_1} E_{i,:}$, where $E_{i,:}$ is the i -th row of E . Then, the agent i computes a stochastic gradient $\sum_{j \in \mathcal{J}_L} \nabla_{u^{(i)}} \hat{f}_\varepsilon^{(i,j),t}$ (Zhao et al., 2014) and update $u^{(i)}$ via

$$u^{(i),t+1} \leftarrow u^{(i),t} + \eta_t \sum_{j \in \mathcal{J}_L} \nabla_{u^{(i)}} \hat{f}_\varepsilon^{(i,j),t}. \quad (13)$$

Here, η_t is the learning rate in the t -th iteration. We set $\eta_t = \frac{\eta}{\sqrt{t+1}}$, where η is the initial learning rate. The dual variables in the target agents can be updated in a similar way. Applying the above steps iteratively till the dual variables converge, each source agent i can compute and store the local

dual objectives $\{\hat{f}_\varepsilon^{(i,j)}\}_{j=1}^J$ based on the information received during the iterations. Accordingly, the source agent i can compute the EOT distance $\widetilde{W}_\varepsilon(\mu, \gamma)$ by collecting $\{\{\hat{f}_\varepsilon^{(i',j)}\}_{j=1}^J\}_{i' \neq i}$ from other source agents. Finally, the source agent i broadcasts $\widetilde{W}_\varepsilon(\mu, \gamma)$ to all other agents.

Algorithm 2 shows the MRBCD scheme, in which the communication complexity per step is given in red. In particular, when updating the dual variables, the communication cost per iteration is $\sum_{i \in I_L} N_i + \sum_{j \in J_L} M_j$. When the numbers of samples in different agents are comparable, i.e., $N_i = \mathcal{O}\left(\frac{N}{T}\right)$ and $M_j = \mathcal{O}\left(\frac{M}{J}\right)$, the communication complexity per iteration can be represented as $\mathcal{O}(L\left(\frac{N}{T} + \frac{M}{J}\right))$. Accordingly, the overall communication complexity for updating dual variables is $\mathcal{O}(TL\left(\frac{N}{T} + \frac{M}{J}\right))$, where T is the number of iterations. When $L = J$, we compute the gradient $\nabla_{u^{(i)}} F_\varepsilon = \sum_{j=1}^J \nabla_{u^{(i)}} \hat{f}_\varepsilon^{(i,j)}$ exactly, and Algorithm 2 becomes the classic randomized block-coordinate descent (RBCD) (Nesterov, 2012). When $L = 1$, we only consider the exchange of dual variables between an agent pair in each iteration. This setting is suitable for the agent with limited computation power because each iteration only involves a pair of agent. This MRBCD scheme is privacy-preserving, which only transmits dual variables, local dual objectives, and the approximated EOT distance. In summary, Figure 2 illustrates the proposed decentralized EOT method.

Essentially, Algorithm 2 is a decentralized and mini-batch stochastic implementation of the randomized block-coordinate descent (RBCD) method Nesterov (2012); Richtárik & Takáč (2014); Lu & Xiao (2015). Therefore, following the Theorem 3 in Wang & Banerjee (2014b), we analyze the convergence error of Algorithm 2 as follows:

- **Assumption 3.** The gradient norm is bounded, i.e., $\|\nabla_{u,v} F_\varepsilon\|_2 \leq R$ for some $R > 0$.

Lemma 3. *For the problem in equation 8 with approximated kernel \widehat{K} , let $(u^*, v^*) \in \mathcal{C}^*$ be the optimal solution in the optimal solution set and $\{(u^t, v^t)\}$ be the sequence generated by Algorithm 2. Define $R_0 = \min_{u,v \in \mathcal{C}^*} \|(u^0, v^0) - (u, v)\|_2$, $\hat{u}^t = \frac{1}{t} \sum_{\ell=1}^t u^\ell$, and $\hat{v}^t = \frac{1}{t} \sum_{\ell=1}^t v^\ell$. Based on the assumption 3, we have*

$$\mathbb{E}|F_\varepsilon(\hat{u}^t, \hat{v}^t; \widehat{K}, E) - F_\varepsilon(u^*, v^*; \widehat{K}, E)| \leq \mathcal{O}\left(\frac{IJ((\sqrt{t} + L_{F_\varepsilon})R_0^2 + \sqrt{t}R^2)}{t}\right), \quad (14)$$

where L_{F_ε} denotes the Lipschitz constant of the objective function F_ε and the expectation is calculated with respect to the randomly-selected agents.

3.3 Theoretical error bound of decentralized EOT

The proposed decentralized EOT method is theoretically-guaranteed. We take the convergence error of the MRBCD algorithm, the optimal loss caused by the approximated kernel, and the mismatch between the storage and communication protocols into account, deriving the bound of the expected approximation error under mild assumptions. In particular, let $\mu = \sum_i p_i \mu_i$ and $\gamma = \sum_j q_j \gamma_j$ be the two distributions in a distributed system with I source agents and J target agents, whose storage and communication protocols are $p \otimes q = [p_i q_j]$ and $E = [e_{ij}]$, respectively. We scatter N samples of μ to the source agents and M samples of γ to the target agents. The kernel matrix of the samples is approximated via Algorithm 1, with the hyperparameter P . As a consequence of Theorem 1, Theorem 2, and Lemma 3, we have

Theorem 4. *For the problem in equation 8 with the kernel \widehat{K} derived by Algorithm 1, let $\{(u^t, v^t)\}$ be the sequence generated by Algorithm 2. Define $\hat{u}^t = \frac{1}{t} \sum_{\ell=1}^t u^\ell$, $\hat{v}^t = \frac{1}{t} \sum_{\ell=1}^t v^\ell$, and the gap between the storage and communication protocols as σ . Based on the assumptions 1-3, with probability*

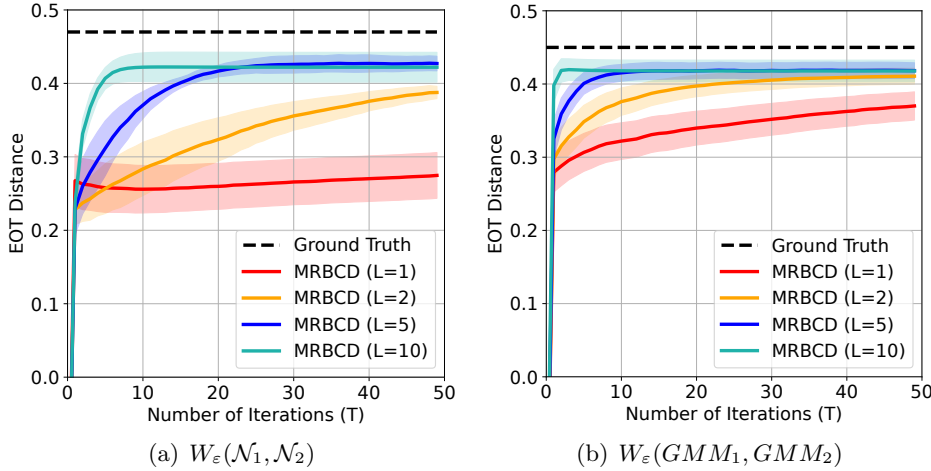


Figure 3: The results for the convergence of our MRBCD scheme.

at least $1 - \delta$, we have

$$\mathbb{E}|F_\varepsilon(\hat{u}^t, \hat{v}^t; \hat{K}, E) - W_\varepsilon(\mu, \gamma)| \leq \mathcal{O}\left(\frac{IJ}{\sqrt{t}} + (N+M)\sqrt{\frac{1}{P} \log \frac{2(N+M)}{\delta}} + \sigma\right). \quad (15)$$

The proof of the theorem is shown in Appendix A.

4 Numerical Experiments

To demonstrate the effectiveness of our decentralized EOT method, we analyze its performance on synthetic data and apply it to distributed domain adaptation tasks. Representative results are shown below. Implementation details and more results are in Appendix B.

4.1 Analytic experiments on synthetic data

We first test the performance of the proposed MRBCD scheme and analyze the influence of the hyperparameter L (i.e., the number of agents used to compute the gradients in each iteration). In particular, we consider two synthetic datasets in this experiment: the first dataset contains two 2D Gaussian distributions ($\mathcal{N}_1, \mathcal{N}_2$), each of which includes 2,000 samples, and the second one contains two 2D Gaussian mixture models (GMM_1, GMM_2), each of which includes two Gaussian components and 2,000 samples. For each dataset, we randomly scatter one distribution's samples to 10 source agents and the other distribution's samples to 10 target agents, respectively. Following the decentralized optimization work in (Zhang & Zhu, 2019; Hughes & Chen, 2021), we assume the network of the agents to be connected, i.e., there always exists a route between two arbitrary agents. Accordingly, the storage and communication protocols are uniform distributions. The kernel matrix is approximated with $P = 1000$. We approximate $W_\varepsilon(\mathcal{N}_1, \mathcal{N}_2)$ and $W_\varepsilon(GMM_1, GMM_2)$ via our MRBCD scheme, in which $L \in \{1, 2, 5, 10\}$, and compare the results with the ground truth achieved by the centralized Sinkhorn algorithm Cuturi (2013). Figure 3 visualizes the convergence of our scheme with different L 's. We can find that with the increase of L , the convergence is faster because the gradients in each iteration are computed with less uncertainty. When $L \geq 2$, our method can approximate the EOT distance with a small gap after sufficient iterations.

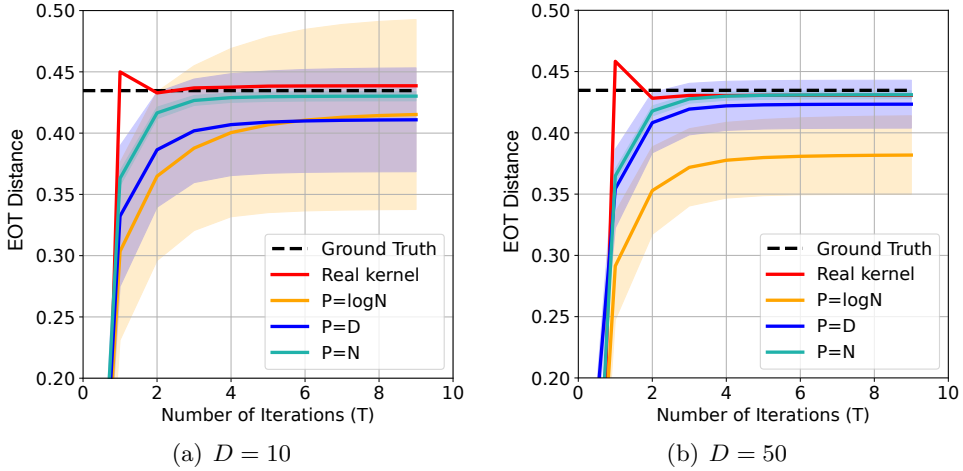


Figure 4: The results corresponding to different kernel matrices. In this experiments, we set $L = 5$ for our MRBCD scheme.

The influence of kernel approximation. The approximation errors shown in Figure 3 are mainly caused by the approximated kernel (when $L \geq 2$). To verify this claim, we decouple the influence of algorithmic convergence and that of kernel approximation, applying our MRBCD scheme with the real kernel matrix and approximated kernel matrix, respectively. In this experiment, we consider computing the EOT distance between two Gaussian distributions, each containing 2,000 samples. By setting $P \in \{\log N, D, N\}$, where $N = 2000$ is the number of samples per distribution and $D \in \{10, 50\}$ is the dimension of the samples, we approximate the kernel matrix with different precision and apply our MRBCD accordingly. Experimental results are shown in Figure 4. When applying the real kernel matrix, our MRBCD method converges quickly, with results close to the ground truth. When $P = N$, the kernel matrix can be approximated with high accuracy, and thus, the results are almost the same as those obtained under the real kernel matrix. When $P = D$, although the performance of our method degrades, the gap between our result and the ground truth can be small for high-dimensional cases. Note that, $D \approx \log N$ when $D = 10$ and $N = 2000$, so the corresponding results in Figure 4(a) are similar.

Remark. Figures 3 and 4 show an interesting phenomenon — although there are one hundred agent pairs in the system, our method converges quickly within 50 iterations and approaches the ground truth. One potential reason for this phenomenon is that all dual variables can be updated based on few agent pairs, i.e., considering $\{(i, j)\}_{i=1}^I$ for an arbitrary target agent j and $\{(i, j)\}_{j=1}^J$ for an arbitrary source agent i . Note that, estimating the EOT distance with few agent pairs is equivalent to estimating the EOT distance with few pairwise costs. Following this direction, the work in (Li et al., 2023) leverages the importance sparsification strategy to solve the primal-form EOT problem with a sparse cost matrix. The theoretical connection between our method and the importance sparsification is left as our future work.

The influence of communication protocol. The communication protocol also impacts our method, as shown in Theorem 4. In Figure 5(a), we apply our method with three different communication protocols: *i*) the ideal communication protocol, i.e., $E = p \otimes q = [\frac{1}{IJ}]$, *ii*) a sparse E , i.e., each source agent only communicate with five target agents (50% zeros in E), and *iii*) a sparse and asymmetric E , i.e., setting the upper-triangular part of the sparse E to be all-zero (directed communication). Experimental results show that the deterioration of the communication environment leads to performance degradation.

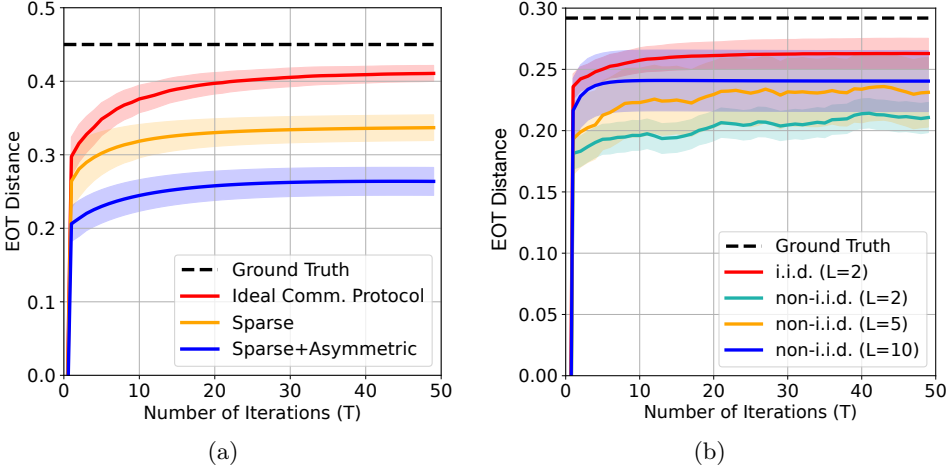


Figure 5: (a) The influence of communication protocol when computing $W_\varepsilon(GMM_1, GMM_2)$. We set $L = 2$ and $P = 1000$ in this experiment. (b) The comparison for i.i.d. and non-i.i.d. data storage methods when computing $W_\varepsilon(GMM_1, GMM_2)$. We set $E = p \otimes q = [\frac{1}{IJ}]$ and $P = 1000$ in this experiment.

The influence of non-i.i.d. data storage. In previous experiments, we randomly scatter the samples to different agents. Accordingly, for the agents in the same domain, their data are independent and identically distributed (i.i.d.). In practice, however, the agents may store non-i.i.d. data. For example, given two Gaussian mixture models, each of which contains five Gaussian components, we *i*) make each agent store the data randomly sampled from the GMMs (i.e., i.i.d. data storage) and *ii*) make each agent store the data from a single Gaussian component (i.e., non-i.i.d. data storage). As shown in Figure 5(b), the non-i.i.d. data storage leads to the degradation of the performance — the gaps between our results and the ground truth become more significant, and the convergence curves are not stable. This phenomenon is because when computing the stochastic gradients of the dual objective, we need to select L agents' dual variables randomly. In the non-i.i.d. case, the stochastic gradients we get are not unbiased estimations of the full-batch gradients unless L equals the number of agents. As a result, compared to the i.i.d. case, we need to use more agents to compute the gradients in the non-i.i.d. case. The results in Figure 5(b) verify our analysis — increasing L can improve the performance in the non-i.i.d. case.

4.2 Real-world distributed domain adaptation

Besides testing on synthetic data, we apply our method to real-world distributed domain adaptation tasks in which the data in the source and target domains are scattered among different agents rather than stored in the same server. Suppose we further protect the privacy of the target domain by preventing the source domain from accessing the data of the target domain. The problem is even more challenging in that case, and existing domain adaptation methods become inapplicable.

We conduct this experiment on two widely-used image datasets, USPS and MNIST (LeCun et al., 1998), each of which has ten image categories corresponding to the digits from 0 to 9. We follow the setting in (Courty et al., 2017a). Given 2,000 images of the MNIST domain and 1,800 images of the USPS domain, we consider the adaptation in two directions: USPS→MNIST and MNIST→USPS. We focus on the OT-based domain adaptation strategy (Courty et al., 2017b). This strategy *i*) computes the (entropic) optimal transport distance between the source and target

Table 1: Comparisons on classification accuracy in distributed domain adaptation tasks

Structure	Method	USPS → MNIST	MNIST → USPS	Preserve Privacy
Source only	1NN	0.385	0.593	Yes
Centralized	EMD	0.544	0.617	No
	Sinkhorn	0.437	0.620	No
	OT-LpL1	0.490	0.676	No
Decentralized (Ours)	MRBCD $_K$	0.580	0.681	No
	MRBCD \hat{K}	0.522	0.629	Yes

domains, *ii*) maps the source samples to the target domain via the optimal coupling, and *iii*) trains the 1-Nearest Neighbor (1NN) classifier based on the mapped data in a distributed manner. To obtain the optimal coupling, we apply various methods, including our MRBCD scheme with real or approximated kernel matrix, the earth mover distance (EMD) for OT distance, the Sinkhorn algorithm for EOT distance, and the OT-LpL1 method in (Courty et al., 2014).

Experimental results in Table 1 show that without the information of the target domain, purely training a 1NN classifier leads to unsatisfactory performance. The traditional centralized OT methods can improve classification accuracy. Still, they require a powerful central server to compute the OT distance and need to access the raw data of the target domain. Our MRBCD scheme outperforms the baselines when using the real kernel and achieves privacy preservation with tolerable performance degradation when using the approximated kernel. In summary, our decentralized EOT has the potential to distributed domain adaptation tasks in challenging privacy-preserving scenarios.

5 Conclusion

In this study, we proposed a decentralized mini-batch randomized block-coordinate descent scheme to approximate the EOT distance in a decentralized scenario and analyzed the approximation error in theory. Our method is privacy-preserving and communicate-efficient, which provides a potential solution to the privacy-preserving distributed distribution comparison task. In the future, we plan to accelerate our method based on the importance sparsification and extend it to more challenging scenarios, e.g., approximating the decentralized EOT for continuous distributions and achieving decentralized Gromov-Wasserstein distance.

References

- Agarwal, A. and Duchi, J. C. Distributed delayed stochastic optimization. In *NeurIPS*, 2011.
- Alistarh, D., Grubic, D., Li, J., Tomioka, R., and Vojnovic, M. QSGD: Communication-efficient SGD via gradient quantization and encoding. In *NeurIPS*, 2017.
- Altschuler, J., Weed, J., and Rigollet, P. Near-linear time approximation algorithms for optimal transport via sinkhorn iteration. In *NeurIPS*, 2017.
- Arabluoei, R., Werner, S., Doğançay, K., and Huang, Y.-F. Analysis of a reduced-communication diffusion LMS algorithm. *Signal Processing*, 117:355–361, 2015.

- Arjovsky, M., Chintala, S., and Bottou, L. Wasserstein generative adversarial networks. In *ICML*, 2017.
- Assran, M., Aytekin, A., Feyzmahdavian, H. R., Johansson, M., and Rabbat, M. G. Advances in asynchronous parallel and distributed optimization. *Proceedings of the IEEE*, 108(11):2013–2031, 2020.
- Basu, D., Data, D., Karakus, C., and Diggavi, S. Qsparse-local-SGD: Distributed SGD with quantization, sparsification and local computations. In *NeurIPS*, 2019.
- Benamou, J.-D., Carlier, G., Cuturi, M., Nenna, L., and Peyré, G. Iterative bregman projections for regularized transportation problems. *SIAM Journal on Scientific Computing*, 37(2):A1111–A1138, 2015.
- Blondel, M., Seguy, V., and Rolet, A. Smooth and sparse optimal transport. In *AISTATS*, 2018.
- Bond-Taylor, S., Leach, A., Long, Y., and Willcocks, C. G. Deep generative modelling: A comparative review of vaes, gans, normalizing flows, energy-based and autoregressive models. *arXiv preprint arXiv:2103.04922*, 2021.
- Chang, T.-H., Hong, M., and Wang, X. Multi-agent distributed optimization via inexact consensus ADMM. *IEEE Transactions on Signal Processing*, 63(2):482–497, 2015.
- Chang, T.-H., Hong, M., Wai, H.-T., Zhang, X., and Lu, S. Distributed learning in the nonconvex world: From batch data to streaming and beyond. *IEEE Signal Processing Magazine*, 37(3):26–38, 2020.
- Chen, M., Shlezinger, N., Poor, H. V., Eldar, Y. C., and Cui, S. Communication-efficient federated learning. *Proceedings of the National Academy of Sciences*, 118(17), 2021.
- Chen, T., Giannakis, G., Sun, T., and Yin, W. LAG: Lazily aggregated gradient for communication-efficient distributed learning. In *NeurIPS*, 2018.
- Chizat, L., Peyré, G., Schmitzer, B., and Vialard, F.-X. Scaling algorithms for unbalanced optimal transport problems. *Mathematics of Computation*, 87(314):2563–2609, 2018.
- Courty, N., Flamary, R., and Tuia, D. Domain adaptation with regularized optimal transport. In *ECML/EKDD*, 2014.
- Courty, N., Flamary, R., Habrard, A., and Rakotomamonjy, A. Joint distribution optimal transportation for domain adaptation. In *NeurIPS*, 2017a.
- Courty, N., Flamary, R., Tuia, D., and Rakotomamonjy, A. Optimal transport for domain adaptation. *IEEE Transactions on Pattern Analysis and Machine Intelligence*, 39(9):1853–1865, 2017b.
- Cuturi, M. Sinkhorn distances: Lightspeed computation of optimal transport. In *NeurIPS*, 2013.
- Damodaran, B. B., Kellenberger, B., Flamary, R., Tuia, D., and Courty, N. Deepjdot: Deep joint distribution optimal transport for unsupervised domain adaptation. In *ECCV*, 2018.
- Dempe, S. and Mehlitz, P. Lipschitz continuity of the optimal value function in parametric optimization. *Journal of Global Optimization*, 61(2):363–377, 2015.

- Deshpande, I., Zhang, Z., and Schwing, A. G. Generative modeling using the sliced wasserstein distance. In *CVPR*, 2018.
- Duchi, J. C., Agarwal, A., and Wainwright, M. J. Dual averaging for distributed optimization: Convergence analysis and network scaling. *IEEE Transactions on Automatic Control*, 57(3): 592–606, 2011.
- Dvurechenskii, P., Dvinskikh, D., Gasnikov, A., Uribe, C., and Nedich, A. Decentralize and randomize: Faster algorithm for Wasserstein barycenters. In *NeurIPS*, 2018.
- Farahani, A., Voghoei, S., Rasheed, K., and Arabnia, H. R. A brief review of domain adaptation. In *Advances in Data Science and Information Engineering*, 2020.
- Ganin, Y. and Lempitsky, V. Unsupervised domain adaptation by backpropagation. In *ICML*, 2015.
- Genevay, A., Cuturi, M., Peyré, G., and Bach, F. Stochastic optimization for large-scale optimal transport. In *NeurIPS*, 2016.
- Hammouda, K. and Karray, F. A comparative study of data clustering techniques. *University of Waterloo, Ontario, Canada*, 2000.
- He, K., Zhang, X., Ren, S., and Sun, J. Deep residual learning for image recognition. *CoRR*, abs/1512.03385, 2015. URL <http://arxiv.org/abs/1512.03385>.
- Hughes, J. and Chen, J. Fair and distributed dynamic optimal transport for resource allocation over networks. In *CISS*, 2021.
- Khanduri, P., Yang, H., Hong, M., Liu, J., Wai, H. T., and Liu, S. Decentralized learning for overparameterized problems: A multi-agent kernel approximation approach. In *ICLR*, 2021.
- LeCun, Y., Bottou, L., Bengio, Y., and Haffner, P. Gradient-based learning applied to document recognition. *Proceedings of the IEEE*, 86(11):2278–2324, 1998.
- Li, M., Yu, J., Xu, H., and Meng, C. Efficient approximation of gromov-wasserstein distance using importance sparsification. *Journal of Computational and Graphical Statistics*, 0(ja):1–25, 2023.
- Liu, Y., Xu, W., Wu, G., Tian, Z., and Ling, Q. Communication-censored ADMM for decentralized consensus optimization. *IEEE Transactions on Signal Processing*, 67(10):2565–2579, 2019.
- Lobel, I. and Ozdaglar, A. Distributed subgradient methods for convex optimization over random networks. *IEEE Transactions on Automatic Control*, 56(6):1291–1306, 2010.
- Lu, Y. and De Sa, C. Moniqua: Modulo quantized communication in decentralized SGD. In *ICML*, 2020.
- Lu, Z. and Xiao, L. On the complexity analysis of randomized block-coordinate descent methods. *Mathematical Programming*, 152(1):615–642, 2015.
- Mao, X., Yuan, K., Hu, Y., Gu, Y., Sayed, A. H., and Yin, W. Walkman: A communication-efficient random-walk algorithm for decentralized optimization. *IEEE Transactions on Signal Processing*, 68:2513–2528, 2020.

- Mattei, P.-A. and Frellsen, J. Miwae: Deep generative modelling and imputation of incomplete data sets. In *ICML*, 2019.
- Nedic, A. Distributed gradient methods for convex machine learning problems in networks: Distributed optimization. *IEEE Signal Processing Magazine*, 37(3):92–101, 2020.
- Nedic, A. and Ozdaglar, A. Distributed subgradient methods for multi-agent optimization. *IEEE Transactions on Automatic Control*, 54(1):48–61, 2009.
- Nesterov, Y. Efficiency of coordinate descent methods on huge-scale optimization problems. *SIAM Journal on Optimization*, 22(2):341–362, 2012.
- Peyré, G. and Cuturi, M. Computational optimal transport. *Foundations and Trends® in Machine Learning*, 11(5-6):355–607, 2019.
- Richards, D., Rebescini, P., and Rosasco, L. Decentralised learning with random features and distributed gradient descent. In *ICML*, 2020.
- Richtárik, P. and Takáč, M. Iteration complexity of randomized block-coordinate descent methods for minimizing a composite function. *Mathematical Programming*, 144(1):1–38, 2014.
- Schmitzer, B. Stabilized sparse scaling algorithms for entropy regularized transport problems. *SIAM Journal on Scientific Computing*, 41(3):A1443–A1481, 2019.
- Seguy, V., Damodaran, B. B., Flamary, R., Courty, N., Rolet, A., and Blondel, M. Large scale optimal transport and mapping estimation. In *ICLR*, 2018.
- Shi, W., Ling, Q., Yuan, K., Wu, G., and Yin, W. On the linear convergence of the ADMM in decentralized consensus optimization. *IEEE Transactions on Signal Processing*, 62(7):1750–1761, 2014.
- Shi, W., Ling, Q., Wu, G., and Yin, W. EXTRA: An exact first-order algorithm for decentralized consensus optimization. *SIAM Journal on Optimization*, 25(2):944–966, 2015.
- Shi, Y., Yang, K., Jiang, T., Zhang, J., and Letaief, K. B. Communication-efficient edge AI: Algorithms and systems. *IEEE Communications Surveys & Tutorials*, 22(4):2167–2191, 2020.
- Sinkhorn, R. and Knopp, P. Concerning nonnegative matrices and doubly stochastic matrices. *Pacific Journal of Mathematics*, 21(2):343–348, 1967.
- Smith, V., Forte, S., Chenxin, M., Takáč, M., Jordan, M. I., and Jaggi, M. Cocoa: A general framework for communication-efficient distributed optimization. *Journal of Machine Learning Research*, 18:230, 2018.
- Staib, M., Claici, S., Solomon, J. M., and Jegelka, S. Parallel streaming Wasserstein barycenters. In *NeurIPS*, 2017.
- Stich, S. U., Cordonnier, J.-B., and Jaggi, M. Sparsified SGD with memory. In *NeurIPS*, 2018.
- Tang, Z., Shi, S., and Chu, X. Communication-efficient decentralized learning with sparsification and adaptive peer selection. In *ICDCS*, pp. 1207–1208, 2020.
- Terelius, H., Topcu, U., and Murray, R. M. Decentralized multi-agent optimization via dual decomposition. *IFAC Proceedings Volumes*, 44(1):11245–11251, 2011.

- Titouan, V., Courty, N., Tavenard, R., and Flamary, R. Optimal transport for structured data with application on graphs. In *ICML*, 2019.
- Uribe, C. A., Dvinskikh, D., Dvurechensky, P., Gasnikov, A., and Nedić, A. Distributed computation of wasserstein barycenters over networks. In *CDC*, 2018.
- Venkateswara, H., Eusebio, J., Chakraborty, S., and Panchanathan, S. Deep hashing network for unsupervised domain adaptation. In *2017 IEEE Conference on Computer Vision and Pattern Recognition (CVPR)*, 2017.
- Villani, C. *Optimal transport: old and new*, volume 338. 2009.
- Wang, H. and Banerjee, A. Bregman alternating direction method of multipliers. In *NeurIPS*, 2014a.
- Wang, H. and Banerjee, A. Randomized block coordinate descent for online and stochastic optimization. *arXiv preprint arXiv:1407.0107*, 2014b.
- Xie, Y., Wang, X., Wang, R., and Zha, H. A fast proximal point method for computing exact wasserstein distance. In *UAI*, 2020.
- Xu, P., Wang, Y., Chen, X., and Tian, Z. Coke: Communication-censored decentralized kernel learning. *Journal of Machine Learning Research*, 22(196):1–35, 2021.
- Ye, J., Wu, P., Wang, J. Z., and Li, J. Fast discrete distribution clustering using wasserstein barycenter with sparse support. *IEEE Transactions on Signal Processing*, 65(9):2317–2332, 2017.
- Yuan, K., Ling, Q., and Yin, W. On the convergence of decentralized gradient descent. *SIAM Journal on Optimization*, 26(3):1835–1854, 2016.
- Zhang, M., Chen, L., Mokhtari, A., Hassani, H., and Karbasi, A. Quantized frank-wolfe: Communication-efficient distributed optimization. *arXiv preprint arXiv:1902.06332*, 2019.
- Zhang, R. and Zhu, Q. Consensus-based distributed discrete optimal transport for decentralized resource matching. *IEEE Transactions on Signal and Information Processing over Networks*, 5(3):511–524, 2019.
- Zhao, T., Yu, M., Wang, Y., Arora, R., and Liu, H. Accelerated mini-batch randomized block coordinate descent method. In *NeurIPS*, 2014.
- Zhu, S., Hong, M., and Chen, B. Quantized consensus ADMM for multi-agent distributed optimization. In *ICASSP*, 2016.

A Delayed Proofs

A.1 The proof of Theorem 1

Proof. Let $u_1, v_1 = \arg \sup_{u,v \in \mathcal{C}(\mathcal{X})} \mathbb{E}_{(i,j) \sim E} [\mathbb{E}_{x \sim \mu_i, y \sim \gamma_j} [f_\varepsilon(x, y, u, v)]]$ be the optimal dual functions of $W_\varepsilon(\mu, \gamma)$. Similarly, let u_2, v_2 be the optimal dual functions of $\widetilde{W}_\varepsilon(\mu, \gamma)$. We have

$$\begin{aligned} |\widetilde{W}_\varepsilon(\mu, \gamma) - W_\varepsilon(\mu, \gamma)| &\leq \begin{cases} \sum_{i,j} (e_{ij} - p_i q_j) \mathbb{E}_{x \sim \mu_i, y \sim \gamma_j} [f_\varepsilon(x, y, u_1, v_1)] & \text{if } \widetilde{W}_\varepsilon(\mu, \gamma) \geq W_\varepsilon(\mu, \gamma) \\ \sum_{i,j} (p_i q_j - e_{ij}) \mathbb{E}_{x \sim \mu_i, y \sim \gamma_j} [f_\varepsilon(x, y, u_2, v_2)] & \text{if } \widetilde{W}_\varepsilon(\mu, \gamma) < W_\varepsilon(\mu, \gamma) \end{cases} \\ &\leq \sum_{i,j} |e_{ij} - p_i q_j| \max_{u \in \{u_1, u_2\}, v \in \{v_1, v_2\}} \mathbb{E}_{x \sim \mu_i, y \sim \gamma_j} [f_\varepsilon(x, y, u, v)] \\ &\leq \sum_{i,j} |e_{ij} - p_i q_j| \sup_{u,v \in \mathcal{C}(\mathcal{X})} \mathbb{E}_{x \sim \mu_i, y \sim \gamma_j} [f_\varepsilon(x, y, u, v)] \\ &= \sum_{i,j} |e_{ij} - p_i q_j| W_\varepsilon(\mu_i, \gamma_j) \\ &\leq \max_{i,j} W_\varepsilon(\mu_i, \gamma_j) \sum_{i,j} |e_{ij} - p_i q_j| \\ &\leq \tau \sigma. \end{aligned}$$

□

A.2 The proof of Theorem 2

Proof. The proof of this Theorem 2 is based on the Lemma 4.1 in (Khanduri et al., 2021). We aims to approximately calculate a $N \times M$ kernel matrix K , which can be considered as a sub-block matrix of the $(N + M) \times (N + M)$ full kernel matrix base on given $N + M$ data samples. This full kernel matrix can be denoted as $K_{full} \in \mathbb{R}^{(N+M) \times (N+M)}$. The employed privacy-preserving Kernel Approximation algorithm, i.e., **Algorithm 1**, can be considered as a partial version of the Algorithm 1 in (Khanduri et al., 2021). As a result, we can utilize the theoretical result, i.e., Lemma 4.1 in (Khanduri et al., 2021) to estimate the approximate level of $\hat{K}_{full} \in \mathbb{R}^{(N+M) \times (N+M)}$ obtained through the Algorithm 1 in (Khanduri et al., 2021). Based on the assumptions 1-2, with probability at least $1 - \delta$, we have

$$\|K_{full} - \hat{K}_{full}\| \leq G(N + M) \left(\sqrt{\frac{32\pi^2}{P} \log \frac{2(N + M)}{\delta}} + \frac{8\pi}{3P} \log \frac{2(N + M)}{\delta} \right).$$

For the reason that K is a sub-block matrix of K_{full} , so as the approximated \hat{K} with respect to \hat{K}_{full} , Furthermore, based on the assumptions 1-2, with probability at least $1 - \delta$, we have

$$\|K - \hat{K}\| \leq \|K_{full} - \hat{K}_{full}\| \leq G(N + M) \left(\sqrt{\frac{32\pi^2}{P} \log \frac{2(N + M)}{\delta}} + \frac{8\pi}{3P} \log \frac{2(N + M)}{\delta} \right),$$

which indicates the result of this Theorem. □

A.3 The proof of Theorem 4

Proof. Let $\hat{u}^*, \hat{u}^* = \arg \max_{u,v} F_\varepsilon(u, v; \hat{K}, E)$ be the optimal solution of the problem equation 8 given approximated kernel \hat{K} , and $\tilde{u}^*, \tilde{u}^* = \arg \max_{u,v} F_\varepsilon(u, v; K, E)$ be the optimal solution of the problem equation 8 given real kernel K . In order to prove equation 15, we first establish the connections with the algorithmic convergence error, the approximated kernel error and the

mismatch between the storage and communication protocols. In particular, applying the triangle inequality, we have

$$\begin{aligned}
& \mathbb{E} \left[|F_\varepsilon(\hat{u}^t, \hat{v}^t; \hat{K}, E) - W_\varepsilon(\mu, \gamma)| \right] \\
& \leq \mathbb{E} \left[|F_\varepsilon(\hat{u}^t, \hat{v}^t; \hat{K}, E) - F_\varepsilon(\hat{u}^*, \hat{v}^*; \hat{K}, E)| \right] + |F_\varepsilon(\hat{u}^*, \hat{v}^*; \hat{K}, E) - F_\varepsilon(\tilde{u}^*, \tilde{v}^*; K, E)| \\
& \quad + |F_\varepsilon(\tilde{u}^*, \tilde{v}^*; K, E) - W_\varepsilon(\mu, \gamma)| \\
& = \underbrace{\mathbb{E} \left[|F_\varepsilon(\hat{u}^t, \hat{v}^t; \hat{K}, E) - F_\varepsilon(\hat{u}^*, \hat{v}^*; \hat{K}, E)| \right]}_{\text{convergence error by Lemma 3}} + \underbrace{|F_\varepsilon(\hat{u}^*, \hat{v}^*; \hat{K}, E) - F_\varepsilon(\tilde{u}^*, \tilde{v}^*; K, E)|}_{\text{approximated kernel error}} \\
& \quad + \underbrace{|\widetilde{W}_\varepsilon(\mu, \gamma) - W_\varepsilon(\mu, \gamma)|}_{\text{gap by Theorem 1}}.
\end{aligned}$$

The first and third terms in the above equation have been analyzed in Lemma 3 and Theorem 1 respectively. The key issue is to analyze the approximated kernel error term.

Each $f_\varepsilon(x, y, u, v)$ is typically convex and Lipschitz continuous with respect to (u, v) Genevay et al. (2016). The objective function F_ε is Lipschitz continuous with respect to (u, v) . Further based on the definition of $f_\varepsilon^{(i,j)}$, it is obvious that $f_\varepsilon^{(i,j)}$ is a liner function with respect to $\kappa(x_n^{(i)}, y_m^{(j)})$. On the whole, the objective function F_ε can be considered as a linear function with respect to kernel matrix K and thus also is Lipschitz continuous with respect to K . According to Dempe & Mehlitz (2015)[Lemma 3.1], if we model K as the varible of the parametric optimization problem

$$\phi(K) = \max_{u,v} F_\varepsilon(u, v; K, E).$$

We can conclude that the optimal value function $\phi(K)$ with respect to K is L_κ -Lipschitz continuous, i.e.,

$$|F_\varepsilon(\hat{u}^*, \hat{v}^*; \hat{K}, E) - F_\varepsilon(\tilde{u}^*, \tilde{v}^*; K, E)| = |\phi(\hat{K}) - \phi(K)| \leq L_\kappa \|\hat{K} - K\|.$$

As a consequence of Theorem 1, Theorem 2, and Lemma 3, we have that for the problem in equation 8 with the kernel \hat{K} derived by Algorithm 1, let $\{(u^t, v^t)\}$ be the sequence generated by Algorithm 2. Define $\hat{u}^t = \frac{1}{t} \sum_{\ell=1}^t u^\ell$, and $\hat{v}^t = \frac{1}{t} \sum_{\ell=1}^t v^\ell$. Based on the assumptions 1-3, with probability at least $1 - \delta$, we have

$$\begin{aligned}
& \mathbb{E} |F_\varepsilon(\hat{u}^t, \hat{v}^t; \hat{K}, E) - W_\varepsilon(\mu, \gamma)| \\
& \leq \mathcal{O} \left(\frac{IJ((\sqrt{t} + L_{F_\varepsilon})R_0^2 + \sqrt{t}R^2)}{t} \right) + L_\kappa G(N+M) \left(\sqrt{\frac{32\pi^2}{P} \log \frac{2(N+M)}{\delta}} + \frac{8\pi}{3P} \log \frac{2(N+M)}{\delta} \right) \\
& \quad + \tau\sigma \\
& \leq \mathcal{O} \left(\frac{IJ}{\sqrt{t}} + (N+M) \sqrt{\frac{1}{P} \log \frac{2(N+M)}{\delta}} + \sigma \right).
\end{aligned} \tag{16}$$

To emphasis, the second term in equation 16 has close relationship with the number of samples per agent (i.e., N_i and M_j). We propose a worst case analysis, while it can be modified properly with well-designed N_i and M_j .

□

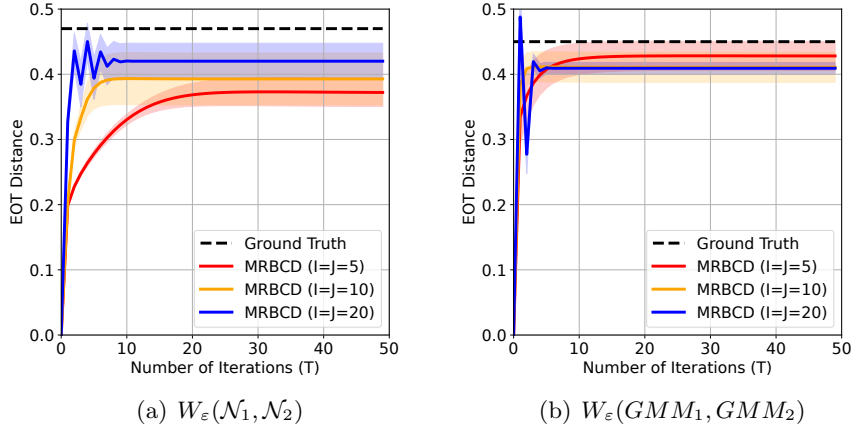


Figure 6: The influence of the number of servers in each domain.

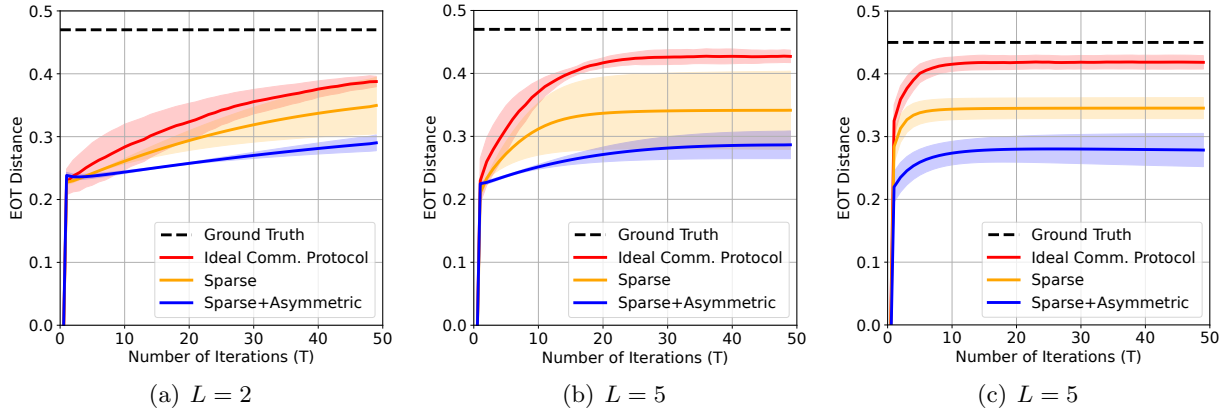


Figure 7: (a, b) The robustness of our method to the communication protocol when computing $W_\epsilon(\mathcal{N}_1, \mathcal{N}_2)$. (c) The influence of communication protocol when computing $W_\epsilon(GMM_1, GMM_2)$. In this experiment, we set $L = 5$ and $P = 1000$.

B Implementation Details and More Experimental Results

B.1 Synthetic experiments

In order to gain insight into the effect of the number of servers on the algorithm, we set $I, J \in \{5, 10, 20\}$, $L = \text{round}(0.7I)$, and the number of samples to be $N = M = 2000$. From the experimental results showed in Figure 6, we can find that as the number of servers increases, convergence is faster at the beginning of the iteration and is accompanied by a more pronounced oscillation.

Additionally, Figure 7 shows more experimental results, visualizing the impacts of different communication protocols.

B.2 Real-world experiments

The distributed domain adaptation task is dedicated to solving the domain adaptation problem in the case where both source and target domain data are scattered over different agents. The aim is to use the label information available in the source domain \mathcal{X} to learn a classifier f^* that can be applied

Table 2: Summary of the domains used in the experiments

Problem	Domains	Datasets	#Samples	#Features	Abbr.
Digits	USPS	USPS	1,800	256	U
	MNIST	MNIST	2,000	256	M
Objects	Art	Office-home	2,427	2,048	Ar
	Clipart	Office-home	4,365	2,048	Cl
	Product	Office-home	4,439	2,048	Pr
	Real-World	Office-home	4,357	2,048	Rw

Table 3: Comparisons on classification accuracy in distributed domain adaptation tasks

Domains	Source only 1NN	Centralized			Decentralized (Ours)	
		EMD	Sinkhorn	OT-LpL1	MRBCD _K	MRBCD _{\hat{K}}
Ar→Cl	0.433	0.471	0.492	0.490	0.483	0.458
Ar→Pr	0.594	0.642	0.673	0.633	0.665	0.639
Ar→Rw	0.667	0.677	0.721	0.686	0.738	0.705
Cl→Ar	0.445	0.504	0.509	0.478	0.531	0.509
Cl→Pr	0.536	0.647	0.617	0.642	0.632	0.606
Cl→Rw	0.589	0.638	0.657	0.664	0.654	0.618
Pr→Ar	0.488	0.516	0.532	0.494	0.538	0.506
Pr→Cl	0.414	0.455	0.465	0.450	0.469	0.425
Pr→Rw	0.683	0.707	0.725	0.714	0.735	0.704
Rw→Ar	0.592	0.611	0.622	0.605	0.621	0.598
Rw→Cl	0.450	0.498	0.505	0.509	0.494	0.463
Rw→Pr	0.729	0.749	0.778	0.770	0.773	0.736

on the target domain \mathcal{Y} without label information. Specifically, suppose we have the source domain data $X_i = \{x_n^{(i)}\}_{n=1}^{N_i}$ associated with the class labels, and the target domain data $Y_j = \{y_m^{(j)}\}_{m=1}^{M_j}$ with unknown labels. Based on our algorithm MRBCD, each target agent j can obtain an optimal coupling $\{\Pi_{ij}\}_{i=1}^I$. Then, according to (Courty et al., 2017a), when the probability measures μ and γ are uniform, we can derive the barycentric mapping as $\widehat{X} = N\Pi Y$, where $\Pi = [\Pi_{ij}]$ is the complete coupling and \widehat{X} is the transported data of the source domain. Eventually, we can train the 1NN classifier f given the transported data \widehat{X} and perform classification prediction on the target domain data.

We further conduct experiments on the object recognition task. Here, we use the Office-home dataset (Venkateswara et al., 2017). A summary of the properties of each domain used in this paper is provided in Table2. The Office-home dataset contains around 15500 images coming from four different domains: Art (artistic images in the form of sketches, paintings, etc), Clipart (collection of clipart images), Product (images of objects without a background) and RealWorld (images of objects captured with a regular camera). For this problem, all the experiments are based on pre-trained ResNet-50 (He et al., 2015). We consider 12 transfer tasks for the Art (**Ar**), Clipart (**Cl**), Product (**Pr**) and Real-World (**Rw**) domains for all combinations of source and target for the 4 domains. The results are shown in the Table3.

Hyperparameter setting. As for the experimental setup, we scattered the source and target domain data over four agents and set $L = 7$ and $P = 10000$. For all the EOT-based method, we apply grid search, finding the optimal weight of regularizer $\varepsilon \in \{2, 1, 0.5, 0.1, 0.05\}$. For our method, the learning rate is set in $\{1, 0.5, 0.1, 0.01, 0.001\}$.